



OPEN ACCESS

EDITED BY

Steven LC Pei,
Yale University, United States

REVIEWED BY

Christian Hanna,
Mayo Clinic, United States
Wolfgang Baehr,
The University of Utah, United States

*CORRESPONDENCE

Hemant Khanna,
hemant.khanna@umassmed.edu,
hemant.khanna@ivericbio.com

†PRESENT ADDRESS

Laura Moreno-Leon,
Iveric Bio, Parsippany, NJ, United States
Hemant Khanna,
Iveric Bio, Parsippany, NJ, United States

SPECIALTY SECTION

This article was submitted to Human and Medical Genomics, a section of the journal Frontiers in Genetics

RECEIVED 30 June 2022

ACCEPTED 25 July 2022

PUBLISHED 19 August 2022

CITATION

Moreno-Leon L, Quezada-Ramirez MA, Bilsbury E, Kiss C, Guerin A and Khanna H (2022), Prenatal phenotype analysis and mutation identification of a fetus with meckel gruber syndrome. *Front. Genet.* 13:982127. doi: 10.3389/fgene.2022.982127

COPYRIGHT

© 2022 Moreno-Leon, Quezada-Ramirez, Bilsbury, Kiss, Guerin and Khanna. This is an open-access article distributed under the terms of the [Creative Commons Attribution License \(CC BY\)](https://creativecommons.org/licenses/by/4.0/). The use, distribution or reproduction in other forums is permitted, provided the original author(s) and the copyright owner(s) are credited and that the original publication in this journal is cited, in accordance with accepted academic practice. No use, distribution or reproduction is permitted which does not comply with these terms.

Prenatal phenotype analysis and mutation identification of a fetus with meckel gruber syndrome

Laura Moreno-Leon^{1†}, Marco A. Quezada-Ramirez¹, Evan Bilsbury¹, Courtney Kiss², Andrea Guerin² and Hemant Khanna^{1*†}

¹Department of Ophthalmology and Visual Sciences, UMass Chan Medical School, Worcester, MA, United States, ²Kingston Health Sciences Centre, Queen's Medical School, Kingston, ON, Canada

Ciliopathies are a class of inherited severe human disorders that occur due to defective formation or function of cilia. The *RPGRIP1L* (retinitis pigmentosa GTPase regulator-interacting protein1-like) gene encodes for a ciliary protein involved in regulating cilia formation and function. Mutations in *RPGRIP1L* cause ciliopathies associated with severe embryonic defects, such as Meckel-Gruber Syndrome (MKS). Here we report *RPGRIP1L* mutation analysis in a family diagnosed with MKS. The clinical manifestations of the fetus included thoraco-lumbar open neural tube defect with associated Chiari type II malformation and hydrocephalus, bilateral club feet, and single right kidney/ureter. Analysis of the parental DNA samples revealed that the father carried a previously reported mutation R1236C/+ whereas the mother had a novel splice site mutation IVS6+1 G > A/+ in *RPGRIP1L*. The splice site mutation resulted in the exclusion of in-frame exon 6 of *RPGRIP1L* (RPGRIP1L-ΔEx6) but expressed a stable protein in fibroblasts derived from the parents' skin biopsies. The GFP-RPGRIP1L-ΔEx6 mutant protein exhibited relatively reduced ciliary localization in transiently-transfected cultured RPE-1 cells. Taken together, this study identifies a novel RPGRIP1L variant RPGRIP1L-ΔEx6, which in combination with RPGRIP1L-R1236C is associated with MKS. We also suggest that the deletion of exon 6 of RPGRIP1L leads to reduced ciliary localization of RPGRIP1L, indicating a plausible mechanism of associated disease.

KEYWORDS

cilia, ciliopathies, *RPGRIP1L*, meckel-gruber syndrome, ciliary defects

Introduction

Cilia are extracellular membrane extensions, which function primarily as sensors to mediate communication between the cell and the extracellular environment (Satir and Christensen, 2007). Disruptions to cilia or cilia anchoring structures leads to a group of pleiotropic genetic disorders called ciliopathies (Hildebrandt et al., 2011). These disorders are characterized by extreme genetic heterogeneity and phenotypic variety. Many of the phenotypic characteristics of these disorders are caused by the disruption of normal cilia function in the process of embryonic development (Eggenchwiler and Anderson, 2007).

Despite the identification of numerous genes involved in ciliopathies the role of these genes in disease is still being delineated.

Meckel syndrome (MKS) and Joubert syndrome (JBTS) are severe, recessive neurodevelopmental disorders caused by mutations in a variety of genes leading to defective primary cilia which disrupts the process of embryonic development (Brancati et al., 2010; Parelkar et al., 2013). Although they are clinically distinct syndromes, there is large genetic/allelic overlap between MKS and JBTS, as well as between these disorders and other ciliopathies such as Bardet-Biedl syndrome (BBS) (Baker and Beales, 2009; Szymanska et al., 2014). The most common clinical features of these disorders are rod-cone dystrophy, post axial polydactyly, neural tube defects (NTD) and renal/genitourinary malformations. The most severe, MKS, is the most common form of syndromic NTD and is neonatally lethal (Logan et al., 2011).

Mutations in 13 genes can account for 75% of all cases of MKS. Among these genes, the most strongly associated with MKS include *CEP290*, *MKS1* and *RPGRIP1L*. Retinitis pigmentosa GTPase regulator-interacting protein-1 like (*RPGRIP1L*), also known as *MKS-5* and *NPHP8*, is a ciliary protein that localizes to the base of the cilium and interacts with retinitis pigmentosa GTPase regulator (*RPGR*) (Arts et al., 2007; Khanna et al., 2009). Essential to the function of *RPGRIP1L* is its ability to localize to the base of the cilium where it controls ciliary gating by maintaining the amount of *CEP290* at the transition zone (TZ) (Wiegering et al., 2021). Disruption of these properties can lead to phenotypes encompassed by MKS and JBTS (Delous et al., 2007; Chen et al., 2011).

Here, we characterize a Canadian family of U.K (paternal) and presumed European descent (maternal) with a history of MKS carrying compound heterozygous variants in *RPGRIP1L*. Identification and characterization of these variations allows for an increased understanding of the pathophysiological processes leading to ciliary dysfunction in MKS and retinal degeneration.

Results

Clinical examination

Routine fetal anatomy ultrasound at 19 weeks revealed a large neural tube defect involving the thoracic spine, ventriculomegaly (measuring 11–15 mm), Chiari malformation, bilateral club feet and two vessel cord/single umbilical artery. Fetal kidneys, cavum septi pellucidi and cisterna magna were unable to be visualized. Amniocentesis was pursued for genetic testing by way of QF-PCR for chromosomes 13, 18, 21 (normal) and sex chromosomes (consistent with a male fetus). Fetal chromosomal microarray analysis did not reveal any clinically significant copy number changes. Fetal whole exome sequencing (including submission of parental samples to perform trio analysis) revealed a paternally inherited *RPGRIP1L* variant

c.706C > T/p.R1236C and a maternally inherited *RPGRIP1L* variant c.776 + 1G > A/IVS6 + 1G > A. No additional variants were reported including no American College of Medical Genetics and Genomics secondary findings. The pregnancy was terminated at 20 weeks 3 days gestation due to the presence of multiple fetal anomalies.

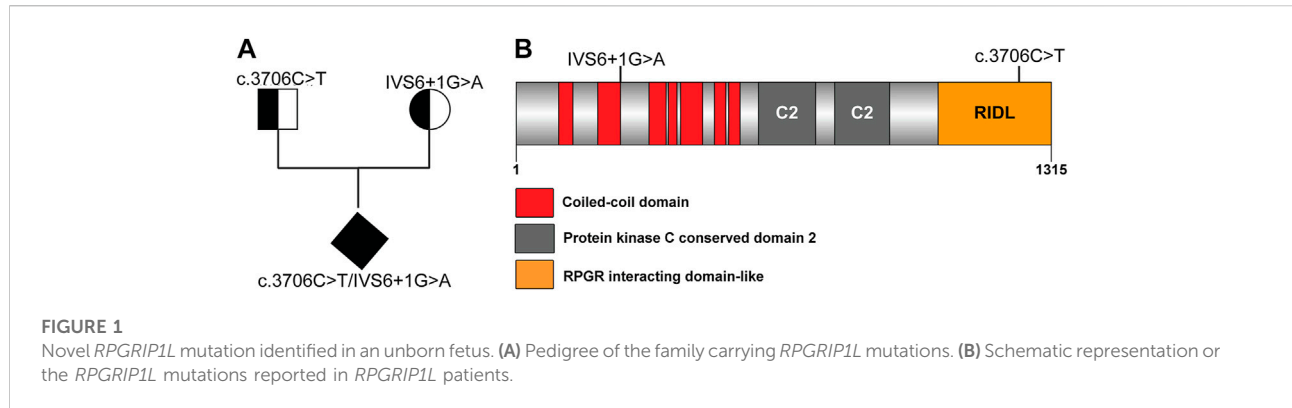
External physical examination of the fetus by geneticist was consistent with an open neural tube defect; mild 5th finger clinodactyly was also present. Fetal autopsy showed thoracolumbar region open neural tube defect, cerebellar tonsillar herniation/Chiari type II malformation, bilateral club feet, imperforate anus, single right kidney/ureter, single or fused midline adrenal gland and two umbilical vessels. Radiological skeletal survey showed multiple formation/segmentation defects evident throughout the spine with widening/dysraphic change apparent within the lower thoracic lumbar and sacral regions. Neuropathological examination showed extensive thoraco-lumbar open neural tube defect with associated Chiari type II malformation and hydrocephalus. We specifically asked about the possibility of molar tooth sign given that this is often a finding in Joubert syndrome and related disorders; neuropathology was unable to confirm or rule out molar tooth sign upon further examination.

Genomic analysis of the *RPGRIP1L* gene in the family

Whole genome sequence analysis of the miscarried fetus identified two potentially disease-associated variants in *RPGRIP1L* (Supplementary Figure S1). The asymptomatic mother carried a heterozygous variant *RPGRIP1L* (NM_015272.2):IVS6+1G > A and the asymptomatic father was heterozygous for *RPGRIP1L* (NM_015272.2):c.3706C > T (R1236C). The fetus, on the other hand had compound heterozygous mutations possessing both variants (Figure 1A). While IVS6+1G > A is located at the donor splice-site between exon 6 (encoding a coiled-coil domain) and intron 6, c.3706C > T (R1236C) is located within the RPGR-interacting domain-like region of *RPGRIP1L* (Figure 1B).

RPGRIP1L expression analysis in fibroblasts

Point mutations in the 5' donor (GT) or 3' acceptor (AG) splice-sites can lead to either exon skipping or intron retention (Baralle, 2005). IVS6+1G > A is located at the exon-intron boundary between exon 6 and intron 6. Splice site prediction analysis revealed that the IVS6+1G > A mutation leads to the loss of the donor splice-site sequence motif by replacing the Guanine residue in the GT consensus sequence with an Adenosine residue (Supplementary Figure S2A). We hypothesized that loss of the 5' donor splice-site at the 5'-end of intron 6 would lead to skipping of exon 6 (Figure 2A). To test this hypothesis, we



generated fibroblasts from skin biopsy specimens of the IVS6+1G > A/+ (mother) as well as control fibroblasts and examined the expression of *RPGRIP1L* mRNA using primer combinations encompassing the splice-site region (Supplementary Table S1 and Figure 2A). RT-PCR analysis using primer pair P1-P3 showed the expression of a shorter PCR product (160 bp) in addition to the expected WT-*RPGRIP1L* (wild type; ~304 bp) product. Sequence analysis of the shorter product revealed a deletion of exon 6 (*RPGRIP1L*-ΔEx 6) (Figure 2B). No change in the PCR profile of *RPGRIP1L* was observed in the R1236C/+ parent fibroblasts.

We next performed quantitative RT-PCR (qRT-PCR) analysis to ask whether the identified variants affect the mRNA levels of *RPGRIP1L* in parents' fibroblasts (Figure 2C). As predicted, mRNA was undetectable for the P5-P3 primer combination (encompassing the mutant transcript without exon 6) in the control and R1236C/+ fibroblasts. The wild-type and the mutant transcripts with primer pairs P5-P3 (mutant transcript) and P4-P3 (wild-type) were detected at 50% levels in the IVS6+1G > A/+ fibroblasts ($p \leq 0.0001$).

We then performed immunoblotting of protein extracts of parents' fibroblasts using an anti-*RPGRIP1L* antibody (Figure 2D). Bands corresponding to *RPGRIP1L*-ΔEx6 and *RPGRIP1L* were observed in the IVS6+1G > A/+ fibroblasts indicating the production of an aberrant shorter polypeptide. A single band, corresponding to the full-length *RPGRIP1L* protein was observed in the R1236C/+ fibroblasts. The specificity of the *RPGRIP1L* antibody was validated by immunoblotting using the HEK293 cells transiently transfected with plasmids encoding the GFP-fused *RPGRIP1L* WT and mutant proteins (Supplementary Figures S2B,C).

Ciliary localization of *RPGRIP1L*

RPGRIP1L has previously been shown to localize to the BB of cilia and function as a ciliary gatekeeper allowing only certain proteins to cross the TZ (Lin et al., 2018; Wiegering et al., 2021).

To test if the observed variations in *RPGRIP1L* alter its ability to localize to the BB, we transiently transfected hTERT-RPE1 cells with plasmid DNA encoding GFP-fused *RPGRIP1L*-WT, *RPGRIP1L*-ΔEx6 or *RPGRIP1L*-R1236C followed by cilia growth and immunofluorescent staining using acetylated tubulin (AcTub; cilia marker), γ -tubulin (γ -Tub; BB marker), and GFP antibodies (Figure 3A). Consistent with previous reports (Arts et al., 2007), *RPGRIP1L*-WT and *RPGRIP1L*-R1236C co-localized with γ -Tub to the BB of the cilia in ~70% of the cells (arrows in Figure 3A). In contrast, BB localization of *RPGRIP1L*-ΔEx6 was detectable only in ~40% of the cells (Figure 3B; $p \leq 0.001$). Quantification of the BB/cytoplasm intensity ratio of *RPGRIP1L* showed ~80% reduction in the localization of *RPGRIP1L*-ΔEx6 at the BB ($p \leq 0.0001$) (Figure 3C). A statistically significant reduction ($p \leq 0.01$) in relative intensity ratio was also observed for *RPGRIP1L*-R1236C compared to *RPGRIP1L*-WT (Figure 3C).

Discussion

Several of the known ciliopathy-causing genes either contribute to a recessive form of the disease (such as in MKS) or modulate the penetrance and expressivity of other causative genes. The significant pleiotropy of *RPGRIP1L* is reflected by the multiple names (*MKS5*, *NPHP8*, *JBTS7*) by which it is referred to when involved in distinct disease processes of varying severity (Andreu-Cervera et al., 2021). Even within the spectrum of MKS, pleiotropy exists between different types of mutations; for example, while homozygous truncating mutations of *RPGRIP1L* typically produce MKS it has been shown that the presence of at least one missense mutation can modify the disease severity and lead to less severe and later onset disease (Reiter and Leroux, 2017). Homozygous missense mutations, frameshift, and splice-site mutations in *RPGRIP1L* have been reported in individuals with JBTS, another severe ciliopathy (Devuyst and Arnould, 2008). Additionally, polymorphic variation in *RPGRIP1L* has been shown to be a modifier of retinal

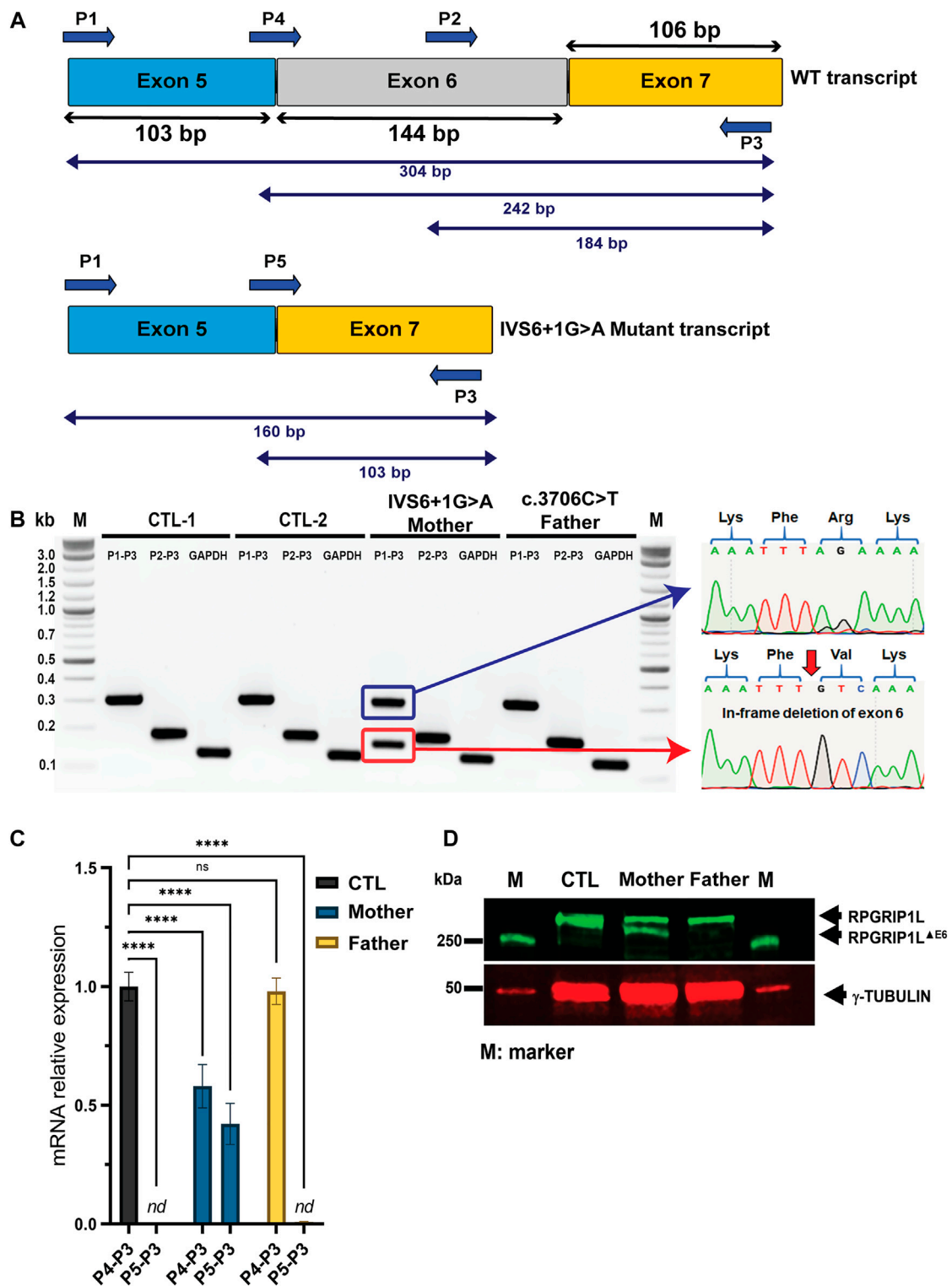
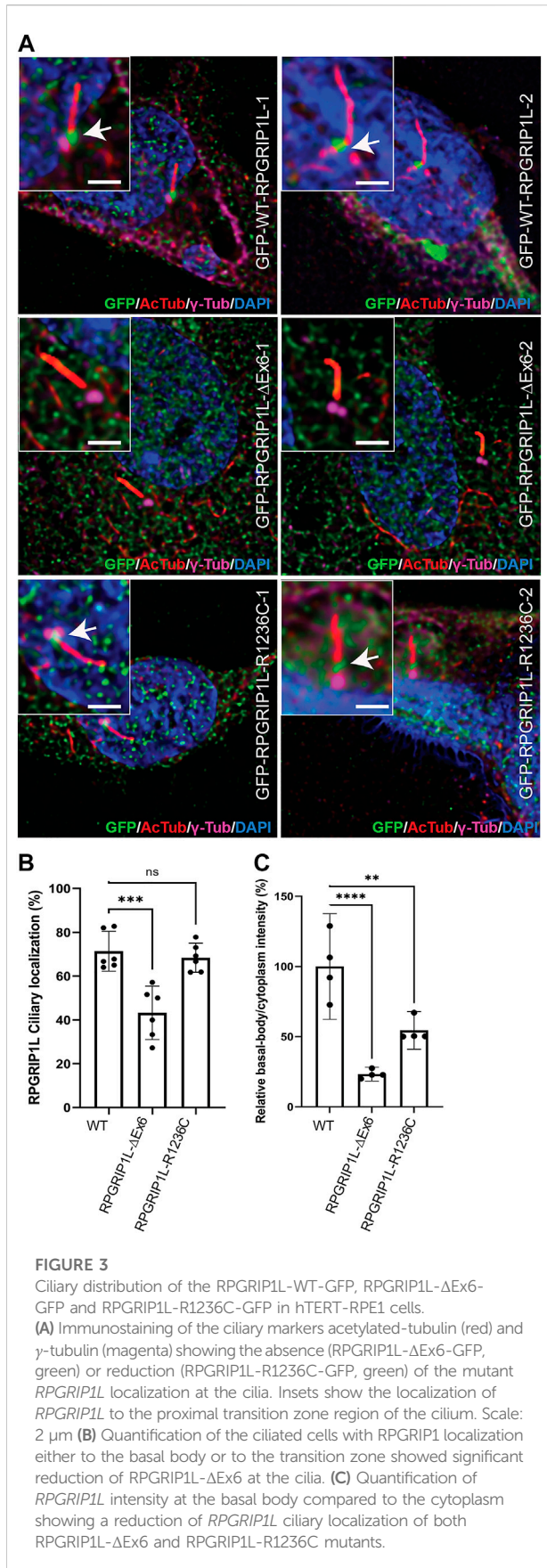


FIGURE 2

Molecular characterization of the novel *RPGRIP1L* IVG6+1G > A mutation in a Canadian family with frequent birth miscarriage. **(A)** Structure of the *RPGRIP1L* gene flanking the IVG6+1G > A mutation with exons size drawn to scale and predicted alternative splicing. Lower panel illustrates the anticipated exon 6 skipping. **(B)** RT-PCR analysis using the indicated primer combinations was performed using fibroblasts derived from the mother and father samples as well as two unrelated controls (CTL-1 and CTL-2). A shorter transcript (~160 bp; red box) was detected in the mother carrying the splice site variant. Sanger sequencing of the aberrant product confirmed the exclusion of exon 6. **(C)** Quantification of the exon 6-skipped *RPGRIP1L* isoform was performed by qRT-PCR analysis. The results are analyzed from three independent experiments. *nd*, non detectable. **(D)** Immunoblotting using *RPGRIP1L* antibody (green) and γ -tubulin (red) showing skipping of exon 6 (*RPGRIP1L*- Δ Ex6) leads to the expression of an aberrant shorter polypeptide in the fibroblasts derived from the mother.



degeneration in ciliopathies (Khanna et al., 2009). Understanding the molecular basis for the varying severity of these mutations is essential for the accurate prediction of phenotypes *via* genetic screenings in the future.

Exon 6 of *RPGRIP1L* encodes a coiled-coil domain. Coiled-coil domains have previously been shown to act as “tags” for oligomerization, notably, of the BBS2 and BBS7 subunits of the BBSome, which is an octameric protein complex involved in regulating protein trafficking at the basal body (BB) of primary cilia (Chou et al., 2019). The BBSome is thusly named because 7 of the eight proteins involved are known causes of Bardet-Biedl syndrome (BBS), another ciliopathy characterized by rod-cone dystrophy, polydactyly, and kidney dysfunction. In addition to this, the coiled-coil domain of exon 6 in *RPGRIP1L* has been shown to be necessary for the proper localization of CEP290 to the transition zone (Li et al., 2016).

Our results show that exon 6 is necessary for proper localization of *RPGRIP1L* to the TZ. There are 7 coiled-coil domains in the protein all of which may engage in oligomerization at the TZ. In *C. elegans*, it has been shown that MKS-5 (mammalian RPGRIP1L/RPGRIP1 orthologue) is crucial for the assembly of a ciliary transition zone and is required for the correct localization of all known *C. elegans* transition zone proteins (Jensen et al., 2015). Jensen et al. were able to demonstrate that the coiled-coil domains of *C. elegans* MKS-5 were, in fact, sufficient for transition zone localization of the protein through truncation studies. This suggests a similar role of the coiled-coil domain of exon 6 in human *RPGRIP1L*.

MKS displays an autosomal recessive (AR) inheritance pattern and parents are usually not aware that they are carriers until after they have an affected child. Once pathogenic variants have been identified in a family, it is possible to prenatally diagnose the disorder using chorionic villus sampling or amniocentesis (Watson et al., 2016). Alternatively, some families may proceed with assisted reproductive technologies such as *in vitro* fertilization with pre-implantation genetic testing for monogenic disease (IVF with PGT-M) to avoid having an affected pregnancy. However, the identification of pathogenic variants is often hindered by an incomplete understanding of the role of different alleles within previously identified causative MKS genes. Currently, the genetic and molecular mechanisms which lead to MKS are known in only ~60% of cases (Szymanska et al., 2012). It has been documented that in some cases, multiple allelism at a single locus or within a single gene can account for some of this phenotypic variability (Chang et al., 2006; Chen, 2007). Recently novel compound variants have been reported in CEP290 (Peng et al., 1935), and aggregating results regarding mutations in *MKS1* have resulted in a proposed genotype-phenotype correlation linking the severity of mutations and the domains affected to diagnoses of either MKS, JBTS or BBS (Leitch et al., 2008; Luo et al., 2020;

Lin et al., 2022). Further studies are needed to not only understand the genotype-phenotype correlation in ciliopathies but also formulate efficient genetic testing so that counseling can be provided to families predisposed to developing debilitating ciliopathies. Based on these results, the family was offered assisted reproductive technologies for future pregnancies. They are currently pursuing *in vitro* fertilization with egg donor. The family was counselled regarding all options, including PGT-M.

Methods

Study approval

The skin biopsies were obtained from *RPGRIP1L* patients and previously published unaffected individuals after written informed consent. Written consent was obtained from the family for publication. All procedures followed the Declaration of Helsinki and approved by the Institutional Review Board of the University of Toronto and UMass Chan Medical School.

Plasmid DNA constructs

Plasmids encoding human WT or mutated *RPGRIP1L*s were obtained with cDNA synthesized from parental skin biopsies using SuperScript™ First-Strand Synthesis System for RT-PCR (Life Technologies). The *RPGRIP1L* coding region was amplified with PrimerSTAR GXL polymerase (Takara) and directly cloned into pMiniT vector (New England Biolabs). The thermal cycle setting was: 98°C for 2 min (activation), 98°C for 10 s and 68°C for 6 min (annealing/extension), for a total 40 cycles. Subsequently, *RPGRIP1L* was subcloned into pEGFP-C1 to express N-terminal GFP-tagged proteins under the control of CMV promoter. Primer details are provided in [Supplementary Table S1](#).

Fibroblast isolation, cell culture and transient transfection

The skin biopsies were dissociated as previously described to obtain primary fibroblasts (Shimada et al., 2017; Moreno-Leon et al., 2020). Briefly, biopsies were washed in iodine followed by three washes in phosphate-buffered saline (Invitrogen). The sample was minced with a sharp scalpel in a culture plate and incubated with Dulbecco's-modified Eagle's medium (DMEM)/F12 (Gibco) supplemented with 20% fetal bovine serum (FBS) (Sigma-Aldrich, Saint-Louis, MO, United States), penicillin and streptomycin at 37°C in a humidified 5% CO₂ incubator. Ten days after harvesting, the

skin was removed, and fibroblasts were passaged for storage and analysis.

Dissociated primary fibroblasts and hTERT-RPE1 cells (ATCC, CRL-4000) were grown in DMEM/F12 media (Gibco) while HEK293 cells were grown in DMEM media (Gibco), 1% Sodium Pyruvate. All cells were supplemented with 10% FBS (Sigma-Aldrich, Saint-Louis, MO, United States) and grown at 37°C and 5% CO₂ incubator. All analyses were done in the fibroblasts at the same passage stages.

Plasmid DNA transfections were performed using Lipofectamine 2000 (Invitrogen) in HEK293 cells and FuGENE 6 (Promega) in hTERT-RPE1 cells at a 3:1 Transfection Reagent: DNA ratio according to the manufacturer's protocol.

RNA extraction and quantitative reverse transcriptase-polymerase chain reaction analysis

Total RNAs were isolated from primary fibroblasts with QIAzol Lysis Reagent (Qiagen) and precipitated according to the manufacturer's instructions. Reverse transcription was performed with 1 µg of total RNAs using the SuperScript™ First-Strand Synthesis System for RT-PCR (Invitrogen). The resulting cDNA was used to perform DNA amplification using PrimeStar GXL DNA polymerase (Takara) according to manufacturer's instruction. Alternative splicing defects were analyzed by agarose gel electrophoresis. Gene expression analysis was performed using the BioRad CFX96 qPCR instrument and Power SYBR Green PCR Master Mix (Thermo Fisher Scientific). All RT-PCR and RT-qPCR primers are described in [Supplementary Table S1](#).

Immunoblotting

The cells were lysed on ice in Pierce RIPA Buffer (Thermo Scientific) containing Halt™ Protease Inhibitor Cocktail (100X, Thermo Fisher). Lysates were sonicated and centrifugated at 12 000 g for 15 min. Supernatants were quantified and 20 µg of total protein lysate was incubated for 5 min at 95°C with Laemmli sample buffer. Proteins were separated on a 4–20% Mini-PROTEAN® TGX™ Precast Protein Gel (BioRad) and transferred to a nitrocellulose membrane (BioRad). The blots were processed using LI-COR western blotting instructions and blocking, and primary and secondary antibodies solutions were prepared in Intercept Blocking buffer (LI-COR). Primary antibodies were incubated overnight at 4°C and secondary antibodies were incubated at room temperature for 2 h ([Supplementary Table S2](#) for antibodies details and dilution information). Protein expression was detected using LI-COR Odyssey Fc detection system.

Immunofluorescence, microscopy and co-localization analysis

The primary fibroblasts and hTERT-RPE1 cells were plated at 90% confluency on coverslips (AmScope CS-R18-100). Primary fibroblasts were serum-starved for 48 h, 24 h after plating. hTERT-RPE1 cells were serum-starved 24 h post-transfection for 24 h. Cells were fixed in 4% paraformaldehyde/1X Dulbecco's phosphate-buffered saline (DPBS; potassium chloride 0.2 g/L, potassium dihydrogen phosphate 0.2 g/L, sodium chloride 8 g/L and disodium hydrogen phosphate 1.15 g/L) for 10 min, washed three times in DPBS and blocked in DPBS containing 5% normal goat serum and 0.5% Triton X-100 for 1 h. Primary antibody solution was prepared in blocking solution and incubated overnight at 4°C. After washing in DPBS, cells were incubated in blocking solution containing Alexa-488-conjugated and Alexa-546-conjugated (Invitrogen) for 1 h. Finally, cells were washed in DPBS and incubated for 5 min with DAPI for nuclear staining. Coverslips were mounted with Antifade Mounting Media (Vectashield) and all images were visualized over $\times 63$ objective using a Leica DM6 Thunder microscope with a 16-bit monochrome camera.

The IMARIS platform was used to process the two channel intensities simultaneously and to measure the degree of overlap of the two channels. After setting intensity threshold, the basal body marker γ -tubulin was used to define a region of interest and a co-localization channel was built on different z-stacks to obtain the percentage of co-localized signal and intensity. When needed, adjacent optical sections were merged in the z-axis to form a projected image (ImageJ). Signal intensity and Co-localization values were plotted using the GraphPad Prism software.

Statistics

All data are presented as means \pm standard deviation from the mean. Two groups comparison was analyzed by Student's t-tests using the Prism GraphPad software. Multiple groups comparison was performed with one-way analysis of variance. Differences between groups were considered statistically significant if $p < 0.05$. The statistical significance is denoted with asterisks (* $p < 0.05$; ** $p < 0.01$; *** $p < 0.005$; **** $p < 0.001$).

Data availability statement

The original contributions presented in the study are included in the article/Supplementary Material, further inquiries can be directed to the corresponding author.

Ethics statement

The studies involving human participants were reviewed and approved by Kingston Health Science Center. The patients/participants provided their written informed consent to participate in this study.

Author contributions

CK, AG, and HK conceived the study; LM-L, MQ-R, and EB performed the experiments; CK and AG collected patient data; LM-L, MQ-R, EB, CK, AG, and HK wrote the paper.

Funding

This work was supported by a grant from the NIH EY022372 to HK.

Acknowledgments

The authors thank the patients for their generosity and willingness to participate in the study. We also thank the members of the Khanna lab for their support and critique.

Conflict of interest

The authors declare that the research was conducted in the absence of any commercial or financial relationships that could be construed as a potential conflict of interest.

Publisher's note

All claims expressed in this article are solely those of the authors and do not necessarily represent those of their affiliated organizations, or those of the publisher, the editors and the reviewers. Any product that may be evaluated in this article, or claim that may be made by its manufacturer, is not guaranteed or endorsed by the publisher.

Supplementary material

The Supplementary Material for this article can be found online at: <https://www.frontiersin.org/articles/10.3389/fgene.2022.982127/full#supplementary-material>

References

- Andreu-Cervera, A., Catala, M., and Schneider-Maunoury, S. (2021). Cilia, ciliopathies and hedgehog-related forebrain developmental disorders. *Neurobiol. Dis.* 150, 105236. doi:10.1016/j.nbd.2020.105236
- Arts, H. H., Doherty, D., van Beersum, S. E., Parisi, M. A., Letteboer, S. J., Gorden, N. T., et al. (2007). Mutations in the gene encoding the basal body protein RPGRIP1L, a nephrocystin-4 interactor, cause Joubert syndrome. *Nat. Genet.* 39, 882–888. doi:10.1038/ng2069
- Baker, K., and Beales, P. L. (2009). Making sense of cilia in disease: the human ciliopathies. *Am. J. Med. Genet. C Semin. Med. Genet.* 151C, 281–295. doi:10.1002/ajmg.c.30231
- Baralle, M. B. D. (2005). Splicing in action: assessing disease causing sequence changes. *J. Med. Genet.* 42, 737–748. doi:10.1136/jmg.2004.029538
- Brancati, F., Dallapiccola, B., and Valente, E. M. (2010). Joubert Syndrome and related disorders. *Orphanet J. Rare Dis.* 5, 20. doi:10.1186/1750-1172-5-20
- Chang, B., Khanna, H., Hawes, N., Jimeno, D., He, S., Lillo, C., et al. (2006). In-frame deletion in a novel centrosomal/ciliary protein CEP290/NPHP6 perturbs its interaction with RPGR and results in early-onset retinal degeneration in the rd16 mouse. *Hum. Mol. Genet.* 15, 1847–1857. doi:10.1093/hmg/ddl107
- Chen, J., Smaoui, N., Hammer, M. B. H., Jiao, X., Riazuddin, S. A., Harper, S., et al. (2011). Molecular analysis of bardet-biedl syndrome families: report of 21 novel mutations in 10 genes. *Invest. Ophthalmol. Vis. Sci.* 52, 5317–5324. doi:10.1167/iovs.11-7554
- Chen, C.-P. (2007). Meckel syndrome: genetics, perinatal findings, and differential diagnosis. *Taiwan. J. Obstet. Gynecol.* 46, 9–14. doi:10.1016/S1028-4559(08)60100-X
- Chou, H.-T., Apelt, L., Farrell, D. P., White, S. R., Woodsmith, J., Svetlov, V., et al. (2019). The molecular architecture of native BBSome obtained by an integrated structural approach. *Structure* 27, 1384–1394.e4. doi:10.1016/j.str.2019.06.006
- Delous, B. L. M., Salomon, R., Laclef, C., Vierkotten, J., Tory, K., Golzio, C., et al. (2007). The ciliary gene RPGRIP1L is mutated in cerebello-oculo-renal syndrome (Joubert syndrome type B) and Meckel syndrome. *Nat. Genet.* 39, 875–881. doi:10.1038/ng2039
- Devuyt, O., and Arnould, V. J. (2008). Mutations in RPGRIP1L : extending the clinical spectrum of ciliopathies. *Nephrol. Dial. Transpl.* 23, 1500–1503. doi:10.1093/ndt/gfn033
- Eggenschwiler, J. T., and Anderson, K. V. (2007). Cilia and developmental signaling. *Annu. Rev. Cell Dev. Biol.* 23, 345–373. doi:10.1146/annurev.cellbio.23.090506.123249
- Hildebrandt, F., Benzing, T., and Katsanis, N. (2011). Ciliopathies. *N. Engl. J. Med.* 364, 1533–1543. doi:10.1056/nejmra1010172
- Jensen, V. L., Li, C., Bowie, R. V., Clarke, L., Mohan, S., Blacque, O. E., et al. (2015). Formation of the transition zone by Mks5/Rpgr11 establishes a ciliary zone of exclusion (CIZE) that compartmentalises ciliary signalling proteins and controls PIP2 ciliary abundance. *EMBO J.* 34, 2537–2556. doi:10.15252/embj.201488044
- Khanna, H., Davis, E., Murga-Zamalloa, C., Estrada-Cuzcano, A., Lopez, I., den Hollander, A. I., et al. (2009). A common allele in RPGRIP1L is a modifier of retinal degeneration in ciliopathies. *Nat. Genet.* 41, 739–745. doi:10.1038/ng366
- Leitch, C. C., Davis, E. E., Stoetzel, C., Diaz-Font, A., Rix, S., Alfaridhi, M., et al. (2008). Hypomorphic mutations in syndromic encephalocele genes are associated with Bardet-Biedl syndrome. *Nat. Genet.* 40, 443–448. doi:10.1038/ng97
- Li, C., Jensen, V. L., Park, K., Kennedy, J., Garcia-Gonzalo, F. R., Romani, M., et al. (2016). MKS5 and CEP290 dependent assembly pathway of the ciliary transition zone. *PLoS Biol.* 14, e1002416. doi:10.1371/journal.pbio.1002416
- Lin, H., Guo, S., and Dutcher, S. K. (2018). RPGRIP1L helps to establish the ciliary gate for entry of proteins. *J. Cell Sci.* 131, jcs220905. doi:10.1242/jcs.220905
- Lin, T., Ma, Y., Zhou, D., Sun, L., Chen, K., Xiang, Y., et al. (2022). Case report: preimplantation genetic testing for Meckel syndrome induced by novel compound heterozygous mutations of MKS1. *Front. Genet.* 13, 843931. doi:10.3389/fgene.2022.843931
- Logan, C. V., Abdel-Hamed, Z., and Johnson, C. A. (2011). Molecular genetics and pathogenic mechanisms for the severe ciliopathies: insights into neurodevelopment and pathogenesis of neural tube defects. *Mol. Neurobiol.* 43, 12–26. doi:10.1007/s12035-010-8154-0
- Luo, M., He, R., Lin, Z., Shen, Y., Zhang, G., Cao, Z., et al. (2020). Novel compound heterozygous variants in MKS1 leading to Joubert Syndrome. *Front. Genet.* 11, 576235. doi:10.3389/fgene.2020.576235
- Moreno-Leon, L., West, E. L., O'Hara-Wright, M., Li, L., Nair, R., He, J., et al. (2020). RPGR isoform imbalance causes ciliary defects due to exon ORF15 mutations in X-linked retinitis pigmentosa (XLRP). *Hum. Mol. Genet.* 29, 3706–3716. doi:10.1093/hmg/ddaa269
- Parelkar, K. S. V., Sanghvi, B. V., Joshi, P. B., Mundada, D., and Oak, S. N. (2013). Meckel-gruber syndrome: a rare and lethal anomaly with review of literature. *J. Pediatr. Neurosci.* 8, 154–157. doi:10.4103/1817-1745.117855
- Peng, M., Han, S., Sun, J., He, X., Lv, Y., and Yang, L. (1935). Evaluation of novel compound variants of CEP290 in prenatally suspected case of Meckel syndrome through whole exome sequencing. *Mol. Genet. Genomic Med.* 10, e1935. doi:10.1002/mgg3.1935
- Reiter, J. F., and Leroux, M. R. (2017). Genes and molecular pathways underpinning ciliopathies. *Nat. Rev. Mol. Cell Biol.* 18, 533–547. doi:10.1038/nrm.2017.60
- Satir, P., and Christensen, S. T. (2007). Overview of structure and function of mammalian cilia. *Annu. Rev. Physiol.* 69, 377–400. doi:10.1146/annurev.physiol.69.040705.141236
- Shimada, H., Lu, Q., Insinna-Kettenhofen, C., Nagashima, K., English, M. A., Semler, E. M., et al. (2017). *In vitro* modeling using ciliopathy-patient-derived cells reveals distinct cilia dysfunctions caused by CEP290 mutations. *Cell Rep.* 20, 384–396. doi:10.1016/j.celrep.2017.06.045
- Szymanska, K., Berry, I., Logan, C. V., Cousins, S. R., Lindsay, H., Jafri, H., et al. (2012). Founder mutations and genotype-phenotype correlations in Meckel-Gruber syndrome and associated ciliopathies. *Cilia* 1, 18–8. doi:10.1186/2046-2530-1-18
- Szymanska, K., Hartill, V. L., and Johnson, C. A. (2014). Unraveling the genetics of Joubert and meckel-gruber syndromes. *J. Pediatr. Genet.* 3, 65–78. doi:10.3233/PGE-14090
- Watson, C. M., Crinnion, L. A., Berry, I. R., Harrison, S. M., Lascelles, C., Antanaviciute, A., et al. (2016). Enhanced diagnostic yield in Meckel-Gruber and Joubert syndrome through exome sequencing supplemented with split-read mapping. *BMC Med. Genet.* 17, 1–9. doi:10.1186/s12881-015-0265-z
- Wiegner, A., Dildrop, R., Vesque, C., Khanna, H., Schneider-Maunoury, S., and Gerhardt, C. (2021). Rpgr11 controls ciliary gating by ensuring the proper amount of Cep290 at the vertebrate transition zone. *Mol. Biol. Cell* 32, 675–689. doi:10.1091/mbc.E20-03-0190